Wear, *173* (1994) 1–12

The dynamic analysis of stick–slip motion

Chao Gao*, Doris Kuhlmann-Wilsdorf and David D. Makel
Department of Materials Science and Engineering, University of Virginia, Charlottesville, VA 22901 (USA)

(Received January 5, 1993; accepted December 2, 1993)

Abstract

The most widely accepted cause of stick–slip motion is that the static (μ_s) exceeds the kinetic friction coefficient (μ_k), or that μ_k drops rapidly at small speeds. Using a dynamic analysis it is shown that the rate of increase of $\mu_s(t)$ with sticking time is a crucial parameter in addition to the condition of $\mu_s > \mu_k$, and that stick–slip may occur even if μ_k increases with speed V. A general equation is derived which describes the stick–slip amplitude (x_s) in terms of substrate speed V_0, spring stiffness K and damping γ, for an arbitrary $\mu_s(t)$ and a linearized $\mu_k(V)$, in contrast to a set of previous equations derived by Brockley *et al.* for an exponential $\mu_s(t)$ and a linearized $\mu_k(V)$ [1]. Additional equations are developed for the "saturation" speed (V_{ss}), below which x_s is independent of V_0, and also for a critical substrate speed V_c above which the stick–slip amplitude vanishes. At speeds between V_{ss} and V_c the stick–slip amplitude generally decreases with increasing V_0, K and γ. Depending on the detailed conditions, different sliding modes including smooth sliding, near-harmonic oscillation or stick–slip can result. Equations developed in this paper suggest practical methods of reducing or eliminating stick–slip for a general system.

1. Introduction

Stick–slip motion, in which two sliding surfaces cycle between relative rest and motion, is a widely observed phenomenon whose effects range from atomic to macroscopic scale, as well as from delicate instrumentation to daily life [2–9]. The most widely accepted cause for stick–slip is that the static friction coefficient (μ_s) exceeds the kinetic friction coefficient (μ_k), or, more rigorously, that μ_k drops rapidly at small speeds [4,10].

In the general case, μ_s and μ_k can be complicated functions of sticking time and surface speed, respectively. Furthermore, static friction is a constraining force during sticking, while kinetic friction is an applied force during slip. Owing to these complications, stick–slip motion is typically studied by graphical methods [10,11] which give only semi-quantitative results.

Bowden and Tabor [4] analytically treated stick–slip motion in an undamped system for constant μ_k and constant μ_s (greater than μ_k). They showed that for such systems the stick–slip amplitude is exactly proportional to the difference between μ_s and μ_k, regardless of experimental parameters. As they pointed out, however, the commonly held assumption of constant μ_s and μ_k is certainly an over-simplification.

*Present address: Robinson Laboratory Computer Microtribology Center, Ohio State University, Columbus, OH 43210-1107, USA

To deduce the speed dependence of μ_k from stick–slip motion assuming constant μ_s, Sampson *et al.* [12] dealt with the stick–slip problem semi-analytically for both damped and non-damped systems. They concluded that for most sliding surfaces μ_k depends weakly on, and can be linearized with, speed and that μ_s depends on sticking time.

By assuming a linear dependence of kinetic friction on speed and an exponential dependence of static friction on stick time, Brockley *et al.* [1] obtained three coupled equations for the critical substrate speed V_c above which stick–slip motion ceases. To do this, they derived an approximate equation for stick–slip amplitude as a function of substrate speed for low speeds, and then deduced the critical substrate speed by letting the stick–slip amplitude approach zero. Their analysis is flawed, however, by the assumption of very low substrate speeds V_0 compared to the critical speed V_c, since this is only true for stick–slip amplitudes near saturation, not as the stick–slip amplitude approaches zero.

Based on experimental results for different surface geometries and lubricants, Eguchi and Yamamoto [13] proposed an empirical relationship in which the growth rate of the static friction force is proportional to the product of critical substrate speed and the spring constant of the system. Their empirical equation is close to the theoretical equation derived herein, except that

0043-1648/94/$07.00
SSDI 0043-1648(93)06393-I

the present analysis also takes into consideration system damping and the speed dependence of kinetic friction.

In this paper, starting with a general dynamic analysis, it will be shown that $\mu_s > \mu_k$ is a necessary but not sufficient condition for stick–slip motion, that $d\mu_s/dt$ is a crucial parameter, and that stick–slip can occur even if μ_k increases with speed V. Explicit equations based on a general $\mu_s(t)$ and a linearized $\mu_k(V)$ are developed for determining the slip mode, the stick–slip amplitude x_s, the critical substrate speed V_c above which stick–slip ceases, and the saturation substrate speed V_{ss} below which the stick–slip amplitude is constant. Comparisons are also made between the theoretical predictions of these equations and a wide range of experimental observations.

2. Basic mathematical theory of sliding with velocity-dependent friction

2.1. Equation of motion for a general system

Although the present mathematical description was stimulated by experiments conducted with the so-called hoop apparatus, whose essential geometry is shown in Fig. 1(a) [2,14–16], it is equally applicable to other friction measuring systems such as the pin-on-disk tribometer (Fig. 1(b)) or the surface-force apparatus (Fig. 1c). In the last two friction measuring systems a spring force Kx and a friction force $P\mu_k(V)$ act on the assumed point-mass slider. The corresponding equation of motion for the slider is

$$m\frac{d^2x}{dt^2}+\gamma\frac{dx}{dt}+kx=P\mu_k(V_r) \tag{1}$$

where $V_r = V_0 - dx/dt$ is the surface velocity between slider and substrate, γ designates the system damping other than the inter-surface friction, $k = m\omega^2$ is the spring constant with ω the system frequency, and P is the normal force. It should be noted that eqn. (1) applies only to slip phases since static friction is a constraining force.

2.2. Equation of motion for the hoop apparatus

In the hoop apparatus, as shown in Fig. 1(a), an assumed point-mass slider moves on the inner hoop surface in response to the friction force, $mg\cos\theta\,\mu_k(V)$, and the gravitational force, $-mg\sin\theta$, resulting in the following equation of motion during slip phases

$$r\frac{d^2\theta}{dt^2}=g\cos\theta\,\mu_k(V_r)-g\sin\theta \tag{2}$$

with r the hoop radius, V_0 the hoop speed, and $V_r = V_0 - r\,d\theta/dt$ the sliding surface speed.

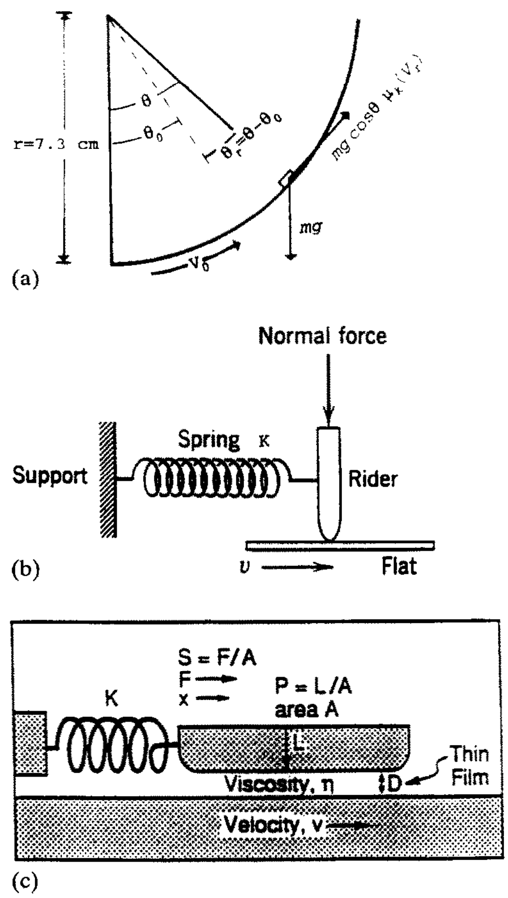

Fig. 1. Schematic diagrams for the dynamics of (a) the hoop apparatus, (b) the pin-on-disc device (adapted from ref. 17, Fig. 4.38), (c) the surface force apparatus (adapted from ref. 28, Fig. 2). K, γ, and V_0 (or V) are the spring constant, the damping coefficient, and the substrate velocity, respectively.

In order to solve eqn. (2), the angular position of the slider is defined in terms of the time-averaged position θ_0 and the displacement away from the time-averaged position θ_r, as shown in Fig. 1(a). When substituting $\theta_r + \theta_0$ for θ, higher orders of θ_r can be neglected because $\theta_r \ll 1$ and $\theta_r \ll \theta_0$, permitting eqn. (2) to be rewritten as

$$\frac{r}{g}\frac{d^2\theta_r}{dt^2}+[\cos\theta_0+\mu_k(V_r)\sin\theta_0]\theta_r+[\sin\theta_0-\mu_k(V_r)\cos\theta_0]=0 \tag{3}$$

2.3. Solution to equation of motion for linearized kinetic friction

In general, $\mu_k(V)$ can be a complicated function of surface speed due to viscous flow, shear thinning, friction heating [4,14,17] and other phenomena, making an analytical solution for either a general system (eqn. (1)) or the hoop apparatus (eqn. (3)) impossible, and thereby requiring the use of graphical or numerical methods. In the context of stick–slip motion, possible effects of chaotic behavior on the motion trajectories can be neglected [11] because of the short time scale of each slip phase.

Equations (1) and (3) are readily solved analytically, and indeed are equivalently the same, if μ_k is assumed to be a linear function of speed, an assumption which was found to be quite satisfactory in an earlier stick–slip analysis [12]. In that case

$$\left[\begin{aligned} \mu_k &= \mu_0+\alpha V_r=\mu_0+\alpha V_0-\alpha\frac{dx}{dt} \\ &= \mu_0+\alpha V_0-\alpha r\frac{d\theta}{dt} \quad \text{for the hoop apparatus} \end{aligned}\right] \tag{4}$$

where μ_0 and α are arbitrary constants. Such a speed dependence of μ_k is shown schematically in Fig. 2(a), where the heavy vertical line at $V_r=0$ denotes the increasing static friction coefficient μ_s as a function of stick time.

Using the linearized form of $\mu_k(V_r)$, eqn. (1) becomes

$$\frac{d^2x}{dt^2}+\frac{\gamma+\alpha P}{m}\frac{dx}{dt}+\omega^2(x-x_0)=0 \tag{5}$$

where $x_0=(\mu_0+\alpha V_0)P/K$ is the time-averaged position.

Again neglecting higher orders of $\theta_r\,d\theta_r/dt=d\theta_r^2/2dt$, eqn. (4) for the hoop apparatus becomes

$$\begin{aligned}\frac{d^2\theta_r}{dt^2}&+\frac{\alpha g}{(1+\tan^2\theta_0)^{1/2}}\frac{d\theta_r}{dt}+\omega^2\theta_r \\ &+\cos\theta_0\,[\tan\theta_0-(\mu_0+\alpha V_0)]=0\end{aligned} \tag{6}$$

where $\tan\theta_0=\mu_0+V_0$ is the time-averaged angular slider position θ_0. While the oscillation frequency for mass–spring systems is defined by $\omega=(K/m)^{1/2}$, in the case of the hoop apparatus the frequency is

$$\begin{aligned}\omega&=\left\{\frac{g}{r}\cos\theta_0[1+(\mu_0+\alpha V_0)\tan\theta_0]\right\}^{1/2} \\ &=\left\{\frac{g}{r}\right\}^{1/2}[1+\mu_k^2]^{1/4}\end{aligned} \tag{7}$$

where we have made use of the facts that $d\theta_r/dt=d\theta/dt$, and $gr\gg V_0^2$, since $r=7.3$ cm and $V_0<5$ cm s^{-1}.

From eqn. (7) we can see that the hoop apparatus furnishes a "spring" without system damping. In the particular experiments cited in this paper, and for a typical value of $\mu_k\approx0.3$, the angular frequency was $\omega\approx11.85$ Hz. By considering the frictionless case, as described by eqn. (7) with $\mu_k=0$, the sliding mode can be recognized as pendulum motion at small angles with a frequency of $\omega=(g/r)^{1/2}$.

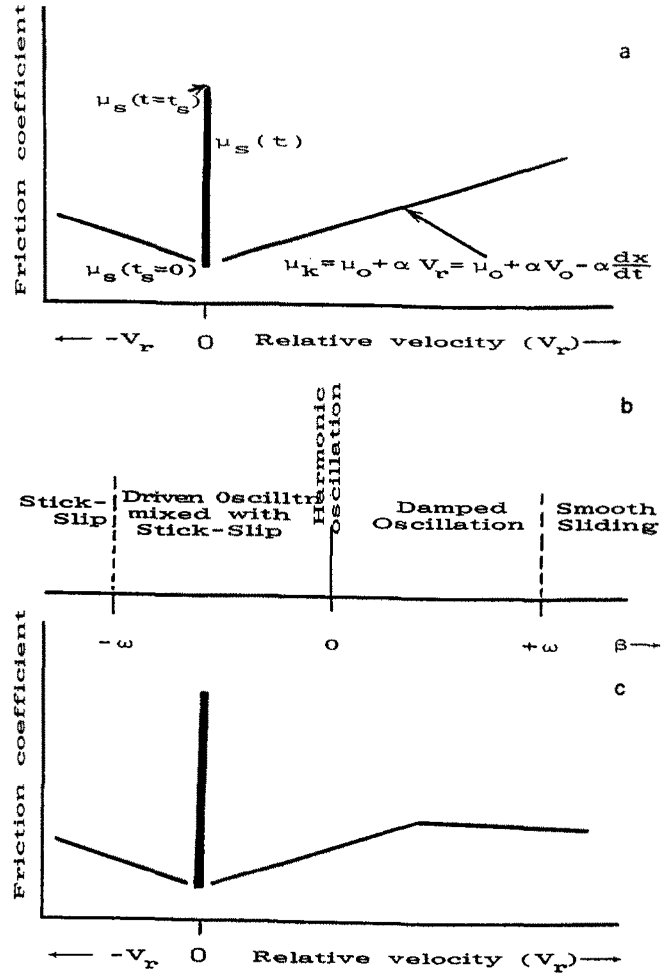

Fig. 2. (a) Schematic graph showing a linear dependence of the kinetic friction coefficient μ_k on the relative velocity V_r between sample velocity V and substrate velocity V_0. Note that the static friction coefficient $\mu_s(V_r=0)$ is a function of stick time t_s and that a positive sample velocity ($V=dx/dt$) decreases V_r by $-dx/dt$. (b) Parameter diagram. Under the assumption of the linear speed dependence shown in (a), the five indicated sliding modes will be observed depending on the parameter $\beta\equiv(\gamma+\alpha P)/2m$ in all friction measuring systems shown in Fig. 1. (c) As (a) but showing a bilinear dependence of the kinetic friction coefficient μ_k on the relative velocity V_r.

Comparing eqns. (5) and (6), one sees that the hoop apparatus is dynamically similar to the general system described by eqn. (5) except that frequency, as given by eqn. (7), is independent of the slider mass, and the system is undamped ($\gamma=0$). Denoting

$$\left[\begin{aligned} \beta &\equiv \frac{\gamma+\alpha P}{2m} && \text{for general systems} \\ \beta &\equiv \frac{\alpha g}{2[1+(\mu_0+\alpha V_0)^2]^{1/2}} && \text{for the hoop apparatus} \end{aligned}\right] \tag{8}$$

the general solution of both eqns. (5) and (6) has the form of

$$\begin{bmatrix} x(t)-x_0=Ae^{\lambda_+t}+Be^{\lambda_-t} & \text{if } |\beta|\neq\omega \\ x(t)-x_0=Ae^{\beta t}+Bte^{\beta t} & \text{if } |\beta|=\omega \end{bmatrix} \tag{9}$$

$$\begin{bmatrix} \lambda_+=-\beta+i(\omega^2-\beta^2)^{1/2} \\ \lambda_-=-\beta-i(\omega^2-\beta^2)^{1/2} \end{bmatrix} \tag{10}$$

where A and B are determined from the initial conditions and x_0 is the time-averaged slider position. As can be seen from eqns. (9) and (10), the motion in terms of sliding mode depends on the relative magnitudes of the various parameters.

3. Application of the equations to different modes of sliding

Figure 2(b) summarizes the different sliding modes described by eqns. (9) and (10) according to values of the *effective* damping parameter $\beta\equiv(\gamma+\alpha P)/2m$ (eqn. (8)). Corresponding to different values of λ_+ and λ_- in eqn. (10) (such as positive or negative, real or imaginary), the resulting modes are

$\beta\leqslant-\omega$ stick–slip motion,
$-\omega<\beta<0$ driven oscillation mixed with stick–slip motion,
$\beta=0$ harmonic oscillation,
$0<\beta<\omega$ damped oscillation, and
$\beta\geqslant\omega$ smooth sliding.

Figure 3 shows some experimental examples of these modes as observed using the hoop apparatus, namely

(a) smooth sliding at 0.5 cm s^{-1} hoop speed and 25% relative humidity (RH), corresponding to the case of $\beta\geqslant\omega$,
(b) near-harmonic motion at 2.8 cm s^{-1} hoop speed and 62% RH, *i.e.* approximating $\beta=0$ for large sliding speeds,
(c) stick–slip at 0.05 cm s^{-1} hoop speed and 62% RH for $\beta<-\omega$ at small sliding speeds,
(d) negative stick–slip at 0.15 cm s^{-1} in air after prolonged testing in a vacuum of 0.04 Torr, indicating $\beta>\omega$ at small sliding speeds but $\beta<0$ at large sliding speeds, and
(e) irregular stick–slip.

A fiber slider was used for (a) through (d) and a solid slider for (e).

The above sliding modes are related through eqns. (4) and (8) to the speed dependence of μ_k as follows:

Case 1. When μ_k is constant in cases of no system damping ($\alpha=0$ in eqn. (6)), or when μ_k *decreases* with increasing speed so as to counterbalance the system damping, *i.e.* $\alpha=-\gamma/P$ in eqn. (5), β vanishes, $\lambda_+=i\omega$, $\lambda_-=-i\omega$, and the slider executes harmonic oscillations (see Fig. 3(b)). The only effect of a constant or slowly decreasing friction force is to shift the time-averaged position of the oscillation by a distance equal to μ_0P/K in the direction of substrate motion.

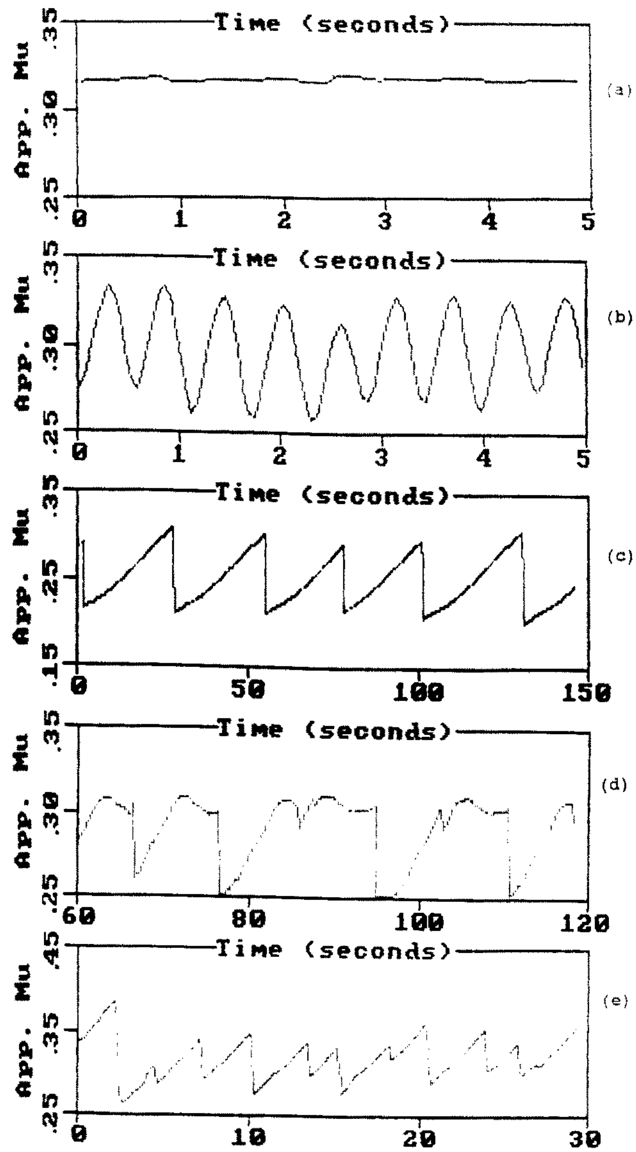

Fig. 3. Experimental traces of $\mu(t)$ under different conditions, all for a gold-plated copper fiber slider on gold-plated copper in the hoop apparatus, except for (e) which refers to a solid slider. (a) Smooth sliding at 0.5 cm s^{-1} hoop speed and at 25% humidity, corresponding to the case of $\beta\geqslant\omega$. (b) Nearly-harmonic oscillation at 2.8 cm s^{-1} hoop speed and 62% humidity, *i.e.* approximating $\beta=0$ for large speeds. (c) Stick–slip motion at 0.05 cm s^{-1} hoop speed and 62% humidity, meaning $\beta<0$ for small speeds. (d) Negative stick–slip at 0.15 cm s^{-1} hoop speed in air, immediately after a prolonged testing in a vacuum of 0.04 Torr, indicating $\beta>\omega$ at small sliding speeds but $\beta<0$ at large sliding speeds. (e) Irregular stick–slip motion of a solid slider at 0.15 cm s^{-1} hoop speed and 68% humidity. The load was 0.5 N in all cases.

Case 2. When the kinetic friction coefficient μ_k *increases* slowly with increasing sliding speed so that $0<\alpha<(2m\omega/P-\gamma/P)$, β is positive and $\beta^2<\omega^2$. Then $\lambda_+=-\beta+\mathrm{i}(\omega^2-\beta^2)^{1/2}$ and $\lambda_-=-\beta-\mathrm{i}(\omega^2-\beta^2)^{1/2}$ and the motion is that of a damped harmonic oscillator.

Case 3. If μ_k increases with speed fast enough so that $\alpha\geqslant(2m\omega/P-\gamma/P)$, then $\beta\geqslant\omega$. In this case $\lambda_+=-\beta+(\beta^2-\omega^2)^{1/2}<0$, $\lambda_-=-\beta-(\beta^2-\omega^2)^{1/2}<0$ (both λ_+ and λ_- are real and negative) and the motion is exponentially damped, resulting in smooth sliding after any excitation (see Fig. 3(a)). This mode can be understood physically since any momentary increase or decrease in sliding speed is counteracted by an increase or decrease in friction force, respectively. Consequently, the slider moves smoothly with a more or less constant surface speed equal to the substrate speed V_0.

Case 4. When μ_k slowly decreases with increasing speed, *i.e.* $0>\alpha>-(2m\omega/P-\gamma/P)$, then $0>\beta>-\omega$, $\lambda_+=|\beta|+\mathrm{i}(\omega^2-\beta^2)^{1/2}$ and $\lambda_-=|\beta|-\mathrm{i}(\omega^2-\beta^2)^{1/2}$ and the resulting slider motion is that of a driven harmonic oscillator.

Case 5. For a still more rapid decrease of friction with increasing speed, *i.e.* $\alpha\leqslant-(2m\omega/P-\gamma/P)$, then $\beta\leqslant-\omega$. In this case $\lambda_+=|\beta|+(\beta^2-\omega^2)^{1/2}>0$, $\lambda_-=|\beta|-(\beta^2-\omega^2)^{1/2}>0$, and any excitation leads to an exponential increase of both displacement and velocity.

It should be noted here that the above solutions of cases 4 and 5 are formal only, since negative β values either lead to stick–slip motion (Fig. 3(c)) for $\beta\leqslant-\omega$ or to a mixture of both stick–slip and oscillation for $-\omega<\beta<0$ [10]. This complication arises from the physical constraint that using the assumption of a linear decrease of μ_k with speed requires a cut-off speed to prevent the friction force from becoming negative. If this cut-off speed is very small, the situation closely resembles $\mu_s>\mu_k(0)$, since the slider spends only a very short time interval in the low-speed region. As a result it is experimentally very difficult to differentiate between these two situations, as both are dynamically unstable [10,18].

Case 6. The final sliding mode is an unusual type of motion called "negative stick–slip" [14], in which the sample slides smoothly at a fixed position, suddenly slips to a smaller displacement, and then quickly returns to smooth sliding, as shown in Fig. 3(d). This behavior is a result of a μ_k which, as schematically displayed in Fig. 2(c), increases with surface speed at low speeds (smooth sliding) but decreases at slightly higher and statistically achievable sliding speeds. An increase and then decrease in friction with increasing sliding speed can be the result of viscous flow of fluid films about contact spots at low speeds followed by shear-thinning at higher speeds [14,16,19], or alternatively by a speed-induced transition from dry to full lubrication [17], as may be caused by the softening of surface layers through friction heating.

4. General considerations on stick–slip motion

The analysis up to this point has considered only the slip phase. Stick–slip motion as a whole can be treated in terms of a general motion trajectory $x(t)$, shown in Fig. 4, where during stick episodes the slider velocity equals that of the substrate. In Fig. 4, the relative motion of a slip episode after a stick phase begins at $t=0$ at a displacement of x_{+s}, which is larger than x_0, the time-averaged position. Inertia carries the slider further upwards for a short interval to x_{max}, where its absolute velocity vanishes and then becomes increasingly negative. The maximum relative velocity is reached at the average position x_0 and then diminishes. After reaching a zero absolute velocity at x_{min}, the sample speeds up to the substrate velocity V_0 and the sample sticks to the substrate at a displacement of $x_{-s}<x_0$. The observed stick–slip amplitude is thus $x_s=x_{+s}-x_{-s}$.

Interestingly, the absolute velocity of the slider *can* become larger than the substrate velocity and thus the slider can overshoot the previous sticking point where $V_r=0$, but only in the rare case of $\mu_s>3\mu_k$, as will be shown in Appendix B.

As long as $\mu_s(t_s\rightarrow\infty)<3\mu_k(V_r\rightarrow0)$, so that overshooting does not occur, the slider velocity and displacement are subject to the following boundary conditions: at the stick point $(t=t')$

$$\left[\begin{array}{l} x(A,B,t=t')=x_{-s} \\ \left.\dfrac{\mathrm{d}x}{\mathrm{d}t}\right|_{t=t'}=V_0 \end{array}\right] \tag{11a}$$

and at the separation point $(t=0)$

$$\left[\begin{array}{l} x(A,B,t=0)=x_{+s} \\ \left.\dfrac{\mathrm{d}x}{\mathrm{d}t}\right|_{t=0}=V_0 \end{array}\right] \tag{11b}$$

Total stick time is $t_s=(x_{+s}-x_{-s})/V_0$ and the stick–slip amplitude $x_s=V_0t_s$.

The four equations in eqn. (11) are insufficient to determine the stick–slip amplitude since there are five unknown constants: A, B, x_{+s}, x_{-s}, and t'. The requisite fifth equation is that x_{+s} must also satisfy the force-balance equation at the separation point

$$Kx_{+s}=P\mu_s(t_s) \tag{12}$$

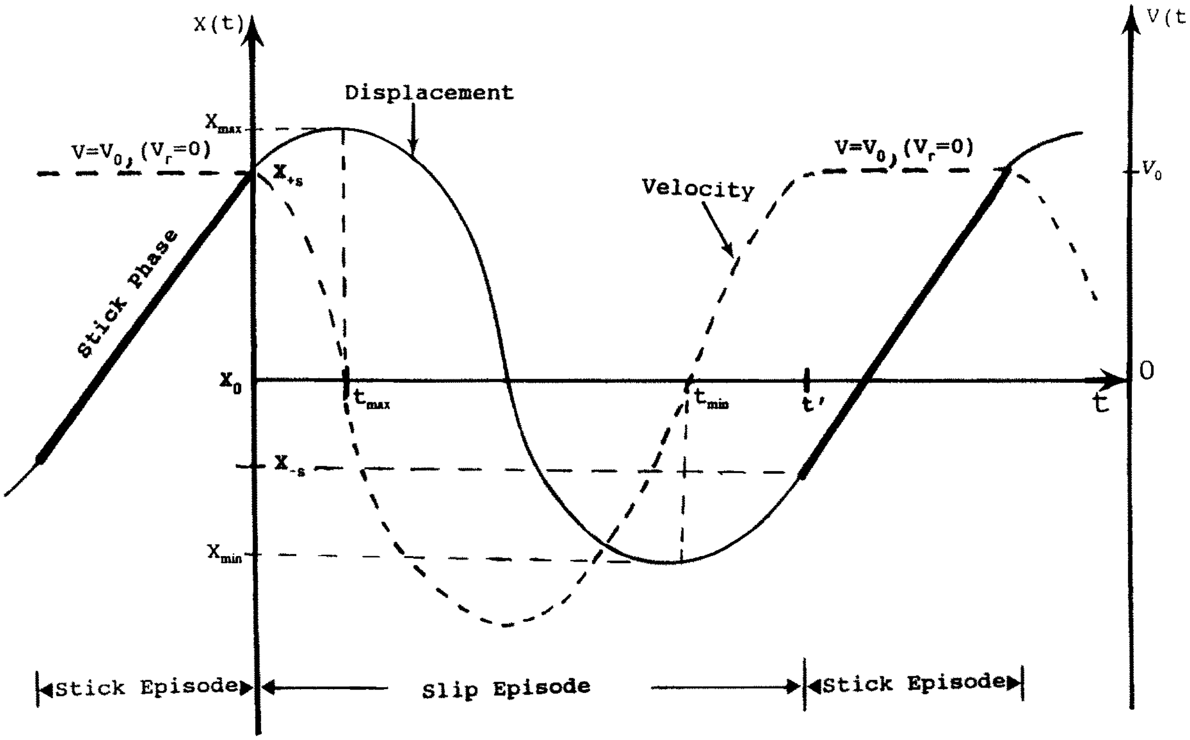

Fig. 4. Schematic illustration of the displacement and velocity in stick–slip motion.

Equation (12), in fact, describes the static friction force on the slider in the stick phase, during which $V_r=0$. In this way the stick–slip amplitude, $x_s=(x_{+s}-x_{-s})=V_0t_s$, can be determined from eqns. (11) and (12) for a general motion trajectory, and no stick–slip will occur if the solution yields x_{-s} equal to or larger than x_{+s}.

5. Stick–slip amplitudes and cessation of stick–slip

5.1. Solving equations for linearized kinetic friction

To illustrate how to derive the stick–slip amplitude for a general form of $\mu_s(t_s)$, consider the example of $\mu_k(V_r)$ described by eqn. (4) (see also Fig. 2(a)) with $|\alpha|<(2m\omega/P-\gamma/P)$. This is case 2 or 4, in which the kinetic friction is a linear, slowly varying function of sliding speed, such that $|\beta|<\omega$ and an analytic trajectory can be found from the equation of motion. Accordingly, the motion is either damped harmonic oscillation if $0<\beta<\omega$ (case 2), or driven oscillation if $0>\beta>-\omega$ (case 4), smooth sliding for $\beta\geqslant\omega$ (case 3), or unstable sliding for $\beta\leqslant-\omega$ (5). With the assumption of μ_k slowly varying with velocity, the motion in the slip phase is readily solved from eqn. (5) or (6) as

$$\left[\begin{array}{l} x(A,B,t)-x_0=e^{-\beta t}(A\cos\Omega t+B\sin\Omega t) \\ \dfrac{dx}{dt}=-e^{-\beta t}[(\beta A-\Omega B)\cos\Omega t+(\Omega A+\beta B)\sin\Omega t] \\ \text{with} \\ \Omega\equiv(\omega^2-\beta^2)^{1/2} \\ x_0=\dfrac{P}{K}(\mu_0+\alpha V_0)=\dfrac{P}{K}\mu_k(V_0) \end{array}\right] \tag{13}$$

Equation (13) represents harmonic motion if $\beta=0$, or near-harmonic motion if $|\beta|\ll\omega$.

Applying eqn. (11b) at $t=0$ (the beginning of the slip episode) to eqn. (13)

$$\left[\begin{array}{l} A=x_{+s}-x_0\equiv x_{+s}-\dfrac{P}{K}(\mu_0+\alpha V_0) \\ B=\dfrac{\beta}{\Omega}+x_{+s}-x_0\equiv \dfrac{\beta}{\Omega}+x_{+s}-\dfrac{P}{K}(\mu_0+\alpha V_0) \\ x(t)-x_0=e^{-\beta t}\left[(x_{+x}-x_0)\cos\Omega t+\dfrac{V_0}{\Omega}\sin\Omega t+\dfrac{\beta}{\Omega}(x_{+s}-x_0)\sin\Omega t\right] \\ V(t)=e^{-\beta t}\left[V_0\cos\Omega t-\dfrac{\beta}{\Omega}V_0\sin\Omega t-\left(1+\dfrac{\beta^2}{\Omega^2}\right)\Omega(x_{+s}-x_0)\sin\Omega t\right] \end{array}\right] \tag{14}$$

Since $dx/dt=0$ at the first turning point, *i.e.* at $t=t_{\max}$, the maximum displacement $x_{\max}=x(t_{\max})$ and maximum speed $V_{\max}=V(t_{\max}+\pi/2\Omega)$ are described by

$$\left[\begin{array}{l} x_{\max}-x_0=\dfrac{e^{-\beta \max}\left[\dfrac{V_0^2}{\Omega}+2\dfrac{\beta^2}{\Omega^2}V_0(x_{+s}-x_0)+\Omega\left(1+\dfrac{\beta^2}{\Omega^2}\right)(x_{+s}-x_0)^2\right]}{\left\{V_0^2+\left[\dfrac{\beta}{\Omega}V_0+\Omega\left(1+\dfrac{\beta^2}{\Omega^2}\right)(x_{+s}-x_0)\right]^2\right\}^{1/2}} \\ \text{with} \\ \operatorname{ctan}\Omega t_{\max}=\dfrac{\beta}{\Omega}+\dfrac{\Omega}{V_0}\left(1+\dfrac{\beta^2}{\Omega^2}\right)(x_{+s}-x_0) \\ V_{\max}=\dfrac{\exp\left[-\beta\left(t_{\max}+\dfrac{\pi}{2\Omega}\right)\right]\left(1+\dfrac{\beta^2}{\Omega^2}\right)}{\left\{V_0^2+\left[\dfrac{\beta}{\Omega}V_0+\Omega\left(1+\dfrac{\beta^2}{\Omega^2}\right)(x_{+s}-x_0)\right]^2\right\}^{1/2}}\left[V_0^2+V_0\beta(x_{+s}-x_0)+\Omega^2(x_{+s}-x_0)^2\right] \end{array}\right] \tag{15}$$

noting that x_{+s} is to be determined from eqn. (12).

Similarly, applying eqn. (11a) at $t=t'$ (the end of the slip episode and the beginning of the stick phase) to eqn. (14)

$$\left[\begin{array}{l} x_{-s}-x_0=-\dfrac{e^{-\beta t'}}{(1+\operatorname{ctan}^2\Omega t')^{1/2}}\left[(x_{+s}-x_0)\left(\operatorname{ctan}\Omega t'+\dfrac{\beta}{\Omega}\right)+\dfrac{V_0}{\Omega}\right] \\ \operatorname{ctan}\Omega t'=-\dfrac{\dfrac{\beta}{\Omega}(x_{+s}-x_0)+\dfrac{\beta}{\Omega}(x_{-s}-x_0)+\dfrac{\Omega}{V_0}\left(1+\dfrac{\beta^2}{\Omega^2}\right)(x_{+s}-x_0)(x_{-s}-x_0)+\dfrac{V_0}{\Omega}}{x_{+s}-x_{-s}} \end{array}\right] \tag{16}$$

Here $\pi\leqslant\Omega t'\leqslant 2\pi$ because sticking can occur only after turning when $t=t_{\min}$.

Ideally, x_{-s} in eqn. (16) and shown in Fig. 4 should be expressed in terms of x_{+s}, which in turn can be determined from eqn. (12). But as one can see from eqn. (16), it is very difficult, if not impossible, to obtain an explicit expression for x_{-s} except in the following cases.

1. In harmonic oscillation, $\beta=0$ (see Fig. 2), $x_{-s}-x_0=-(x_{+s}-x_0)$ by symmetry, and the same solution will approximately hold for near-harmonic oscillation when $|\beta|\ll\omega$.

2. For any value of β, eqn. (15) shows that when $V_0 \to 0$ or $V_0 \ll V_{max}$, $x_{+s} \to x_{max}$, meaning $\Omega t' \to \pi (t_{max} \to 0)$ and there is full stick–slip.
3. Similarly, when $V_0 \to V_{max}$, $x_{+s} \to x_0$, meaning $\Omega t' \to 2\pi$, leading to near-extinction of stick–slip.

Thus, from eqn. (16), we obtain

$$\begin{bmatrix} x_{-s}-x_0=-(x_{+s}-x_0) & \text{if } |\beta| \ll \omega & \text{(for any } V_0) \\ x_{-s}-x_0=-(x_{+s}-x_0)e^{-\beta\pi/\Omega} & \text{if } V_0 \longrightarrow 0 & \text{(full stick-slip)} \\ x_{-s}-x_0=-(x_{+s}-x_0)e^{-2\beta\pi/\Omega} & \text{if } V_0 \longrightarrow V_m & \text{(near no stick-slip)} \end{bmatrix} \tag{17}$$

5.2. *Graphical determination of the stick–slip amplitude*

Calculating the stick–slip amplitude ($x_s = x_{+s} - x_{-s}$) is still difficult, since a mathematical model of static friction as a function of stick time is required, and this is dependent on the model assumptions, as influenced by the specific sliding conditions [2,12,13,20–27]. As an example, Fig. 5 shows experimentally determined curves of μ_s as a function of stick time for a gold-plated copper fiber sample sliding on a gold-plated copper hoop in an atmosphere of humid nitrogen. The interesting feature here is that the initial rate of increase of μ_s apparently rises with increasing applied load. This is in accord with a theoretical model based on the effect of the size of the contact spots [2].

Both theories and experimental observations [2,12,13,20–27] indicate that the static friction coefficient initially increases rapidly with stick time and then levels off asymptotically at long periods of stick, as depicted in Fig. 6. On this basis, we can draw quantitative conclusions regarding the stick–slip amplitude by making use of eqn. (17) to obtain

$$\begin{bmatrix} x_s \equiv s_{+s} - x_{-s} = (x_{+s} - x_0)(1 + e^{-\beta t'}) \\ \text{namely} \\ x_{+s} = x_0 + \dfrac{x_s}{1 + e^{-\beta t'}} \end{bmatrix} \tag{18}$$

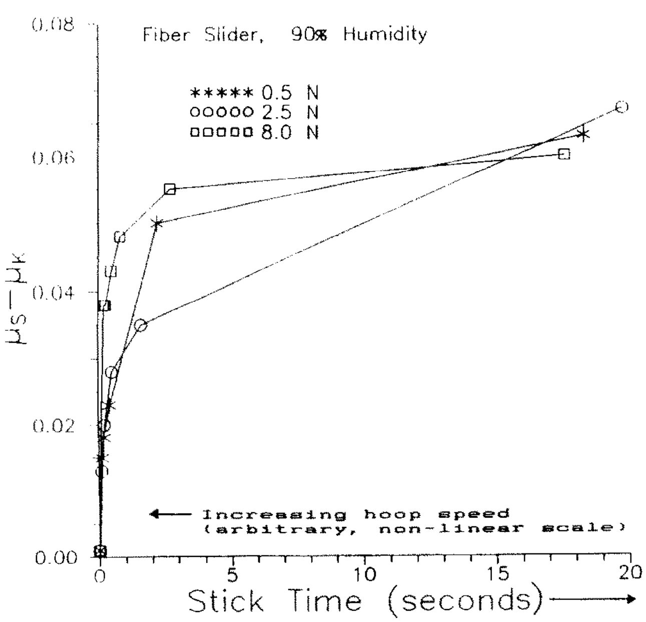

Fig. 5. Experimental data for $\mu_s - \mu_k$ as a function of stick time for three different applied loads as indicated.

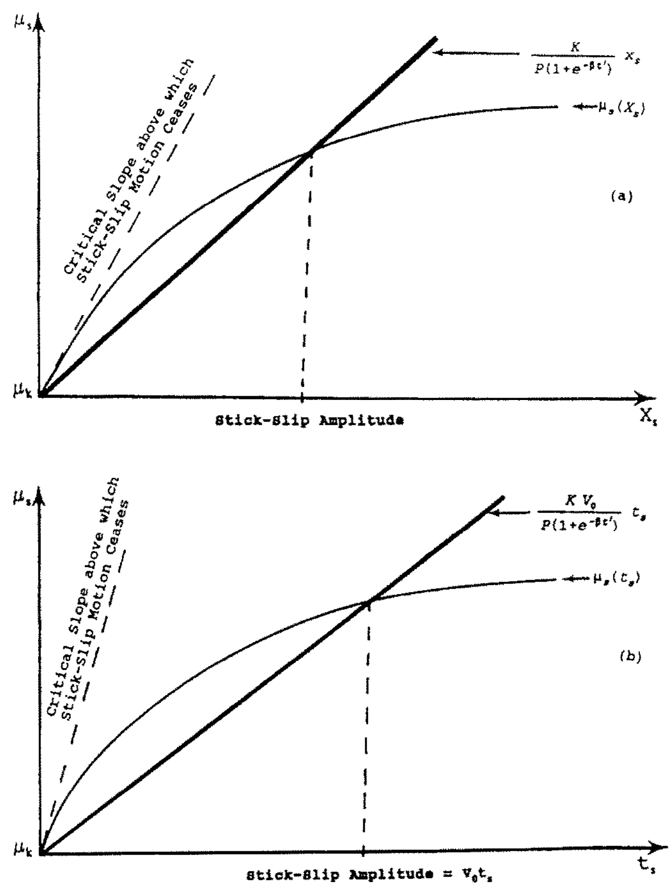

Fig. 6. Graphical method for finding the stick–slip amplitude, x_s, if the time dependence is known (shown here of the type in Fig. 5; also see Fig. 4.42 in ref. 9), according to eqn. (19). (a) Value of x_s at the intercept gives the stick–slip amplitude. (b) Value of t_s at the intercept gives the stick–slip amplitude via $x_s = V_0 t_s$.

Substituting into eqn. (12) gives

$$\left[\begin{array}{l} \dfrac{K}{P(1+e^{-\beta t'})}x_s=\mu_s(x_s)-\mu_k(V_0) \\ \text{namely} \\ \dfrac{KV_0}{P(1+e^{-\beta t'})}t_s=\mu_s(t_s)-\mu_k(V_0) \end{array}\right] \qquad (19)$$

where as previously stated, $Kx_0=P\mu_k(V_0)$, $\Omega t'\rightarrow\pi$ for $V_0\ll V_{max}$ (full stick–slip), and $\Omega t'\rightarrow 2\pi$ for $V_0\rightarrow V_m$ (near-extinction of stick–slip).

For a general dependence of μ_s on stick time, the stick–slip amplitude can now be obtained graphically from eqn. (19) by plotting the left side of the equation as a function of x_s (or t_s), which is a straight line with a constant slope, and by plotting the right side of the equation on the same graph, as shown in Fig. 6. The point of intersection, if any, gives x_s (or t_s), and therefore the stick–slip amplitude, $x_s=V_0t_s$.

5.3. Cessation of stick–slip

As can be seen from Fig. 6(a), at a given substrate speed, increasing K (the stiffness of the spring) rotates the straight line counter-clockwise. Consequently the point of intersection, if present, moves toward the origin, indicating a decreasing stick–slip amplitude. At a critical value of K the two curves meet only at the origin, indicating cessation of stick–slip for this and larger values of K.

Similarly, increasing the substrate speed reduces the stick–slip amplitude. Physically, this is because stick times shorten progressively and there is less time for μ_s to increase. Mathematically, a larger substrate speed increases the slope of the straight line due to a decreasing t_s, as shown in Fig. 6(b). Since μ_s more or less saturates at t_{ss}, $\mu_s(t_{ss})\approx\mu_s(t_\infty)$. Therefore, from eqn. (19), the maximum stick–slip amplitude $x_{ss}=V_0t_\infty=(P/K)(1+e^{-\beta\pi/\Omega})[\mu_s(t_\infty)-\mu_k]$, will be affected very little by substrate speed if $V_0<V_{ss}$. V_{ss} is therefore named the saturation speed, and is defined by

$$V_{ss}=\frac{x_s}{t_{ss}}\approx\frac{P}{Kt_{ss}}\left(1+\exp\left[-\frac{\pi\beta}{(\omega^2-\beta^2)^{1/2}}\right]\right)[\mu_s(t_\infty)-\mu_k] \qquad (20)$$

because the stick time t_s for a substrate speed less than V_{ss} is larger than t_{ss}. For $V_0>V_{ss}$, however, the stick–slip amplitude decreases with increasing substrate speed up to a critical substrate speed, V_c, above which stick–slip motion ceases.

This critical substrate speed can be determined as follows: As can be seen from Figs. 5 and 6, the slope of the μ_s curve reaches its maximum as $t_s\rightarrow 0$, while the straight line has a constant slope. Therefore the two curves will intercept only if

$$\left[\begin{array}{l} \dfrac{K}{P(1+e^{-\beta t'})}\leqslant\left.\dfrac{\partial\mu_s}{\partial x_s}\right|_{x_s\rightarrow 0} \\ \text{namely} \\ \dfrac{KV_0}{P(1+e^{-\beta t'})}\leqslant\left.\dfrac{\partial\mu_s}{\partial t_s}\right|_{t_s\rightarrow 0} \end{array}\right] \qquad (21)$$

When the two sides of each of the equations are equal, $x_s=0$, meaning a zero stick–slip amplitude. Physically, this defines a critical substrate velocity above which no stick–slip occurs. As shown previously, $t'=2\pi/\Omega$ when stick–slip is near extinction. Thus, the critical speed is

$$V_c=\frac{P}{K}(1+\exp\left[-\frac{2\pi\beta}{(\omega^2-\beta^2)^{1/2}}\right]\left.\frac{\partial\mu_s}{\partial t_s}\right|_{t_s\rightarrow 0} \qquad (22)$$

As may be deduced from Fig. 3, this critical speed is on the order of 1 cm s^{-1} in the case of the hoop apparatus tests, and depends on humidity, load and the type of slider.

6. Comparison with experiments

Based on eqns. (19), (20) and (22), and the above discussion, the stick–slip amplitude stays essentially constant as the substrate speed increases from zero to V_{ss} and then decreases until the extinction of stick–slip at V_c. Experimentally, both V_{ss} and V_c have been observed, as reported in the literature [2,13–17,26,28]. In particular, experiments using the hoop apparatus at different loads and humidities (Fig. 7(a)), experiments reported in ref. 17 with a pin-on-disk type system for different spring constants (Fig. 7(b)), and experiments of ref. 13 using a block-on-flat for different lubricants (Fig. 7(c)) show the same features as described in this analysis. Further, eqn. (22) has been empirically determined and experimentally verified by Eguchi and Yamamoto [13] under lubricated conditions for different surface geometries.

The effects of damping ($\beta>0$) or pumping ($\beta<0$) on the stick–slip amplitude can be understood via eqn. (19). In the case of $\beta>0$ (damping) in which μ_k increases with speed slowly or decreases with speed too slowly to cancel the damping term, the effects are that the slope of the straight line in Fig. 6 is increased and the difference between μ_s and $\mu_k(V_0)$ is decreased, both resulting in diminished stick–slip amplitude. In the case of $\beta<0$ (pumping), by contrast, the effects are the opposite, resulting in a larger stick–slip amplitude. Thus, from the relation of $\beta=(\gamma+\alpha mg)/2m$, we can see that $d\mu_k/dV=\alpha<0$ is only one of the cases which will induce

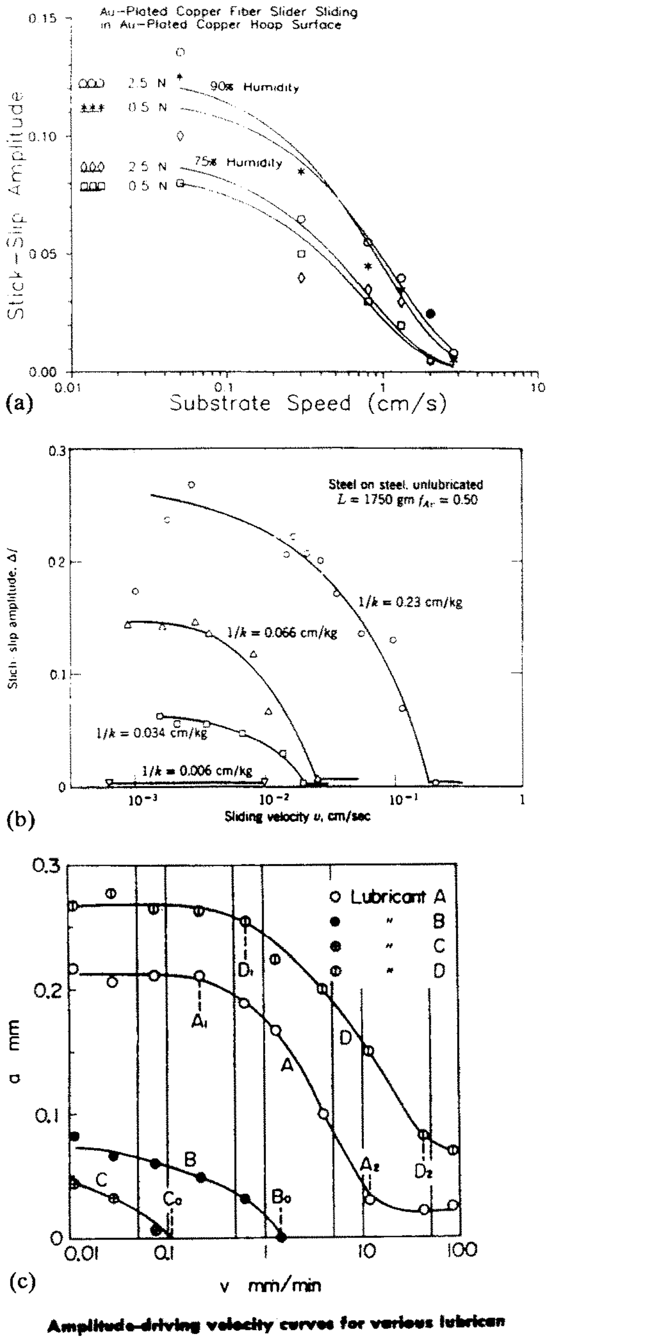

Fig. 7. Experimental stick–slip amplitude as a function of substrate speed: (a) in the hoop apparatus at different humidities and loads, (b) in a pin-on-disk type device for different spring constants according to ref. 17 (Fig. 4.44), (c) in a block-on-flat type system for different lubricants according to ref. 13 (Fig. 6). Note the saturation speed V_{ss} (eqn. (20)) below which the stick–slip amplitude is nearly constant, and the critical speed V_c (eqn. (22)) above which the stick–slip amplitude is practically zero — all of course, depending on the detailed experimental conditions.

stick–slip motion. Indeed, even $d\mu_k/dV \geqslant 0$ may also cause stick–slip motion as long as eqn. (21) is satisfied.

In this manner eqns. (19) to (22) explain why, in practice, increasing the spring stiffness, substrate speed, and/or system damping not only reduces the stick–slip amplitude but also can completely eliminate stick–slip motion, as in the observation noted by Rabinowicz [17].

Finally, two limiting cases are worth noting.

1. If there is no difference between static and kinetic friction, as would be represented by a horizontal line coinciding with the stick time axis in Fig. 6(b), regular stick–slip motion cannot occur since eqn. (21) cannot be satisfied.
2. If μ_s is constant but higher than μ_k, meaning a discontinuity of μ_s or a positive infinitely large slope at $t_s = 0$, eqn. (21) is always satisfied, but stick–slip cannot occur unless the relative speed between the sample and substrate (V_r) equals zero. Otherwise, the motion may be smooth or oscillatory sliding without any sticking and the motion is independent of the properties of μ_s.

7. Conclusions

By means of a dynamic analysis, a complete set of five equations has been derived which describe the stick–slip motion for an arbitrary slip trajectory in terms of the speed dependence of kinetic friction and the time dependence of static friction.

Assuming a linear speed dependence of kinetic friction, equations describing slider trajectory in slip phases for a spring–mass system and for the so-called hoop apparatus have been obtained analytically. The sliding modes are controlled by the effective damping coefficient β (eqn. 8). Smooth sliding occurs for large positive β values, damped harmonic motions for small positive β values, harmonic oscillations for zero β value, driven harmonic oscillations for small negative β values, and unstable sliding (leading to stick–slip) for large negative β values.

For modes other than smooth sliding and for a general static friction $\mu_s(t_s)$, an equation has been derived for calculating the stick–slip amplitude in terms of substrate speed, system frequency and damping, and kinetic and static friction. Based on that equation, the critical speed V_c above which no stick–slip occurs, and the saturation speed V_{ss} below which the stick–slip amplitude is almost independent of the substrate speed have also been determined. Starting at V_{ss}, the stick–slip amplitude decreases with increasing substrate speed until the extinction of stick–slip motion at V_c.

Furthermore, a condition (eqn. (A3)) for which the slider may slip over the previous stick point has been determined as given in Appendix B. Visually, such a slippage may occur only when the stick episode traverses at least the free spring equilibrium position.

This paper has also shown that stick–slip motion does not *necessarily* occur even if static friction is larger than kinetic friction. Rather it depends on detailed experimental parameters such as sliding speed, spring stiffness, and system damping. Above all, stick–slip depends on $d\mu_s/dt$, *i.e.* the rate at which μ_s increases with stick time above its initial value of μ_k, which is determined by the specific sliding conditions. Somewhat surprisingly, stick–slip may occur even if μ_k increases with speed. The system damping γ acts as a positive component of $d\mu_k/dV$ which can be added to the linear term of $\mu_k(V)$, as shown in eqn. (8).

The predictions of this analysis are fully consistent with a wide range of observations on stick–slip amplitude, sliding modes, and critical and saturation speeds, made by this as well as other research groups. Consequently, the equations derived in this analysis are confidently expected to be widely useful for understanding and controlling the different aspects of stick–slip motion in terms of both friction and system properties.

Acknowledgments

The sponsorship of this research through the Materials Division of the Office of Naval Research, Arlington, VA, and the National Science Foundation (Division of Mechanical and Structural Systems, Materials Engineering and Tribology Program, Dr. Jorn Larsen-Basse) is gratefully acknowledged.

References

1 C.A. Brockley, R. Cameron and A.F. Potter, Friction induced vibration, *J. Lubr. Technol., April 1967* 101–108.
2 C. Gao, D. Kuhlmann-Wilsdorf and D.D. Makel, Fundamentals of stick–slip, *Wear, 162–164* (1993) 1139–1149.
3 G.M. McClelland and C. Mate, Atomic scale friction measured with an atomic force microscope, in P.J. Blau and F. Smidt (eds.), *Engineered Materials for Advanced Friction and Wear Applications*, ASM International, Metals Park, OH, 1988, pp. 13–22.
4 F.P. Bowden and D.T. Tabor, *The Friction and Lubrication of Solids*, Clarendon Press, Oxford, 1986.
5 K. Khurana, *Phys. Today 41* (5) (1988) 17.
6 B. Skalmierski, The construction of old Italian violins: tentative explanation, *Bull. Acad. Polon. Sci. (Techniques), 29* (1981) 175–181.
7 Z. Li, E. Rabinowicz and N. Saka, The stiction between magnetic recording heads and thin film disks, *Tribology and Mechanics of Magnetic Storage Systems*, STLE SP-26, 1989, pp. 64–70.
8 F.P. Bowden and D. Tabor, *Friction – An Introduction to Tribology*, Anchor Press/Doubleday, New York, 1973, pp. 68–71.
9 G. Galton, The action of brakes: on the effect of brakes upon railway trains, *Engng, 25* (1878) 469–472.
10 A.A. Andronow and C.E. Chaikin, *Theory of Oscillations*, Princeton University Press, 1949, p.161.
11 K. Popp and P. Stelter, Stick–slip vibrations and chaos, *Phil. Trans. R. Soc. Lond. A, 332* (1990) 89–105.
12 J.B. Sampson, F. Morgan, D.W. Reed and M. Muskat, Studies in lubrication; XII. Friction behavior during the slip portion of the stick–slip process, *J. Appl. Phys., 14* (1943) 689–700.
13 M. Eguchi and T. Yamamoto, Effect of surface geometry on relationship between static friction and stationary contact time in stick–slip oscillation, *Proc. Jpn. Soc. Lubr. Eng., July, 1985* 1053–1058.
14 C. Gao and D. Kuhlmann-Wilsdorf, On stick–slip and the velocity dependence of friction at low speeds, *Trans. ASME, J. Tribol., 112* (1990) 354–360.
15 C. Gao and D. Kuhlmann-Wilsdorf, Adsorption films, humidity, stick–slip and resistance of sliding contacts, *IEEE 1990 Holm Conf. on Electrical Contacts, Montréal, Aug. 20–24, 1990*, IEEE, Piscataway, NJ, pp. 292–300; also in *IEEE Trans. Comp. Hybr. Man. Technol., 14* (1991) 37–44.
16 C. Gao, D. Kuhlmann-Wilsdorf and D.D. Makel, Moisture effects including stiction resulting from adsorbed water films, *Trans. ASME, J. Tribol., 114* (1992) 174–180.
17 E. Rabinowicz, *Friction and Wear of Materials*, Wiley, 1965.
18 D. Karnopp, Computer simulation of stick–slip friction in mechanical dynamic systems, *Trans. ASME, 107* (1985) 100–103.
19 D.M. Heyes, Some physical consequences of large shear rates on simple liquids, *J. Chem. Phys., 85* (1986) 997–1008.
20 B.V. Derjagin, V.E. Push, and D.M. Tolstoi, A theory of stick–slip sliding of solids, *Proc. Conf. Lubrication and Wear, Oct. 1957*, p. 265.
21 P.H. Howe, D.P. Benton and I.E. Puddington, London–Van der Waals attractive forces between glass surfaces, *Can. J. Chem., 6* (1955) 1375.
22 J.I. Kosterin and I.V. Kraghelsky, Relaxation Oscillation in Elastic Friction Systems, *Frict. Wear in Machinery, 12* (1962) 111.
23 F.P. Bowden and D. Tabor, *The Friction and Lubrication of Solids, Part II*, Oxford, 1965, pp. 338–340.
24 C.A. Brockley and H.R. Davis, The time-dependence of static friction, *J. Lubr. Technol., Jan. 1968* 35–41.
25 C. Gao and D. Kuhlmann-Wilsdorf, Experiments on, and a Two-Component Model for, the Behavior of Water Nano-Films on Metals, *MRS Symposium Proc., 188*, Mater. Res. Soc., Pittsburgh, PA, 1990.
26 J.T. Burwell and E. Rabinowicz, The nature of the coefficient of friction, *J. Appl. Phys., 24* (2) (1953) 136–139.
27 S. Kato, N. Sato and T. Matsubayashi, Some considerations on characteristics of static friction of machine tool slideway, *Trans. ASME, J. Lubr. Technol., July 1972* 234–247.
28 M.L. Gee, P.M. McGuiggan and Israelachvili, Liquid to solidlike transitions of molecularly thin films under shear, *J. Chem. Phys., 93* (3) (1990) 1895–1906.

Appendix A: Nomenclature

A	integral constant
B	integral constant
g	acceleration due to gravity
K	spring constant of measuring system
m	sample mass
P	normal force between sample and substrate
r	hoop radius

RH	relative humidity
t	time
t'	time in a slip episode
t_s	time in a stick episode
t_{ss}	time beyond which static friction ceases to grow
t_∞	infinite time
V	absolute sample velocity
V_0	substrate velocity
V_c	critical substrate speed above which stick–slip motion ceases
V_h	hoop velocity
V_r	relative velocity $(V-V_0)$
V_{ss}	saturation substrate speed below which stick–slip amplitude is independent of the substrate speed
x	momentary sample displacement*
x_0	time-average sample displacement
x_{max}	maximum sample displacement
x_{min}	minimum sample displacement
x_s	stick–slip amplitude
x_{-s}	displacement at beginning of a stick episode
x_{+s}	displacement at end of a stick episode
$dx/dt=V$	absolute sample velocity (V)
α	coefficient of the linear term for μ–V curve
β	effective damping coefficient of measuring system
γ	damping coefficient of measuring system
θ	momentary angular position of sample on hoop
θ_0	time-averaged angular position on the hoop
θ_r	difference between momentary and time-averaged angular position $(\theta-\theta_0)$
ω	oscillation frequency in harmonic motion
Ω	oscillation frequency in damped or pumped harmonic motion
$\lambda_\pm$	two roots for second-order auxiliary equation
μ_k	kinetic friction coefficient
μ_s	static friction coefficient

Appendix B

As stated in the text, the slider velocity can become larger than the substrate velocity, and thus the slider can overshoot the previous sticking point where $V_r=0$, but only in the rare case that $\mu_s>3\mu_k$. This is possible because at the point of sticking, where the relative velocity V_r vanished, static friction provides a constraining force which is equal and opposite to the spring force. Normally, at the onset of stick, no net force acts on the slider, resulting in no acceleration or deceleration, and sticking occurs when the velocity of the slider increases to the substrate velocity, *i.e.* when $V_r=0$.

However, in cases of $\mu_s>3\mu_k$, the sample can overshoot the stick point where $V_r=0$. As a simple example of this concept, consider the case of harmonic oscillation, when $\beta=0$ or when μ_k is constant in the absence of system damping (case 1 of the previous section). By symmetry, the difference in displacement between the separation (slip) point and the time-averaged position is the same as that between the stick point and the time-averaged position, *i.e.* $x_{+s}-x_0=-(x_{-s}-x_0)$. Noting that $Kx_0=P\mu_k$ from eqn. (5) and $Kx_{+s}=P\mu_s(t_s)$ at the separation point, we have

$$\mu_s(t_s)+\frac{Kx_{-s}}{P}=2\mu_k \tag{A1}$$

In regard to the position of the stick point, two cases need to be distinguished.

i. The case of sticking at a negative displacement, *i.e.* $x_{-s}<0$, if the restoring force of the spring is larger than the static friction at the instant of stick, *i.e.* if

$$-Kx_{-s}>P\mu_s(t_s=0) \tag{A2}$$

the slider is accelerated toward the spring equilibrium with a velocity larger than the substrate velocity.

ii. For a positive stick point position, *i.e.* of $x_{-s}\geqslant 0$, slippage at the stick point requires that $Kx_{-s}>P\mu_s(t_s=0)$. This, however, is not possible because it is equivalent to requiring at least $\mu_k>\mu_s(0)$, since $Kx_{-s}<Kx_0=P\mu_k$, leading to no stick–slip. Combining eqns. (A1) and (A2), the condition for the slider velocity exceeding the substrate velocity at the "stick" point becomes

$$\mu_s(t_s)-\mu_s(0)>2\mu_k \tag{A3}$$

This can occur only when the motion during the stick episode at least includes the free spring equilibrium position. Assuming $\mu_s(0)=\mu_k$. Equation (A3) may be simply expressed as $\mu_s>3\mu_k$ [12], which is highly unlikely.

*All displacements measured relative to the free spring position